

# LLM-VA: Resolving the Jailbreak-Overrefusal Trade-off via Vector Alignment

Anonymous ACL submission

## Abstract

Safety-aligned LLMs suffer from two failure modes: jailbreak (responding to harmful inputs) and over-refusal (declining benign queries). Existing vector steering methods adjust the magnitude of answer vectors, but this creates a fundamental trade-off—reducing jailbreak increases over-refusal and vice versa. We identify the root cause: LLMs encode the decision to respond (answer vector  $v_a$ ) and the judgment of input safety (benign vector  $v_b$ ) as nearly orthogonal directions, treating them as independent processes. We propose LLM-VA, which aligns  $v_a$  with  $v_b$  through closed-form weight updates, making the model’s willingness to respond causally dependent on its safety assessment—without fine-tuning or architectural changes. Our method identifies vectors at each layer using SVMs, selects safety-relevant layers, and iteratively aligns vectors via minimum-norm weight modifications. Experiments on 12 LLMs demonstrate that LLM-VA achieves 11.45% higher F1 than the best baseline while preserving 95.92% utility, and automatically adapts to each model’s safety bias without manual tuning. Code and models are available at <https://anonymous.4open.science/w/LLM-VA-Web-A6C4/>.

## 1 Introduction

Large language models (LLMs) have achieved remarkable capabilities across diverse NLP tasks (OpenAI, 2024; Team, 2025; AI@Meta, 2024), yet safety alignment remains challenging. Safety-aligned LLMs exhibit two failure modes: *jailbreak*, where the model responds to toxic inputs (i.e., queries designed to elicit harmful, unethical, or unsafe responses) (Yi et al., 2024; Zou et al., 2023b; Yuan et al., 2025), and *over-refusal*, where the model unnecessarily declines benign queries (Röttger et al., 2024; Zhang et al., 2025a; Cui et al., 2025). This dual failure mode significantly limits the deployment of LLMs in safety-

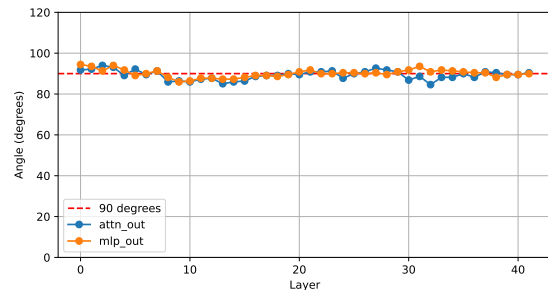


Figure 1: The angles between answer vectors ( $v_a$ ) and benign vectors ( $v_b$ ) are approximately 90° across layers in gemma-2-9b-it, indicating near-orthogonality between response decisions and safety assessments.

critical applications, where both reliability and usability are essential. Among approaches to address these issues, vector steering (Zou et al., 2023a; Arditì et al., 2024; Sheng et al., 2025) has gained attention for its efficiency—it manipulates specific directions in the model’s latent space without costly retraining, using only simple answer/refuse labels rather than fine-grained annotations.

However, existing vector steering methods only adjust the *magnitude* of the answer vector, creating a fundamental trade-off: reducing magnitude suppresses jailbreak but increases over-refusal, while amplifying it has the opposite effect (Arditì et al., 2024; Sheng et al., 2025). Recent methods like SCANS (Cao et al., 2025) and CAST (Lee et al., 2024) incorporate input toxicity but require architectural modifications and treat both failure modes as separate objectives (see Table 1). This magnitude-based paradigm cannot fundamentally resolve the trade-off.

We identify the root cause of this trade-off: existing methods control *output behavior* (answer vs. refuse) without considering *input characteristics* (benign vs. toxic). To investigate, we extract two vectors at each layer: the *answer vector* ( $v_a$ ), indicating whether the model will respond, and the

benign vector ( $v_b$ ), indicating whether the input is safe. As shown in Figure 1, these vectors are nearly orthogonal ( $\sim 90^\circ$ ) across layers,<sup>1</sup> revealing that LLMs treat response decisions and safety assessments as *independent* processes. This explains both failure modes: the model may answer toxic inputs (jailbreak) or refuse benign ones (over-refusal) because its willingness to respond is decoupled from its judgment of input safety.

Based on this observation, we propose Large Language Model Vector Alignment (LLM-VA). By aligning these vectors, we make the model’s willingness to respond *causally dependent* on its safety assessment (Zou et al., 2023a), rather than treating them as independent decisions. Crucially, LLM-VA achieves this through closed-form weight updates—requiring no gradient-based optimization, fine-tuning, or architectural changes. Our method involves three steps:

- **Vector identification via SVMs:** Train SVMs at each layer to find hyperplanes separating benign/toxic and answer/refuse samples, yielding both  $v_b$  and  $v_a$ .
- **Layer selection:** Identify layers most relevant to safety decisions based on their contribution to final output and SVM classification accuracy.
- **Vector alignment:** Adjust layer weights to align  $v_a$  with  $v_b$ , ensuring benign inputs activate the “answer” direction while toxic inputs do not.

Extensive experiments on 12 LLMs demonstrate that LLM-VA achieves 11.45% higher F1 scores (effectiveness on resolving trade-off) than the best baseline (AlphaSteer) (Sheng et al., 2025) with only 4.08% model utility drop, which indicates LLM-VA effectively resolves the jailbreak-overrefusal trade-off while preserving general capabilities. In summary, our contributions are:

- We propose LLM-VA, which, to the best of our knowledge, is the first vector steering method that simultaneously addresses both jailbreak and over-refusal by aligning answer vectors with benign vectors through closed-form weight updates—requiring no gradient-based fine-tuning or architectural changes.
- We demonstrate on 12 LLMs from 5 model families that LLM-VA achieves state-of-the-art safety alignment, and show that it automatically adapts

<sup>1</sup>Results for other LLMs are similar; see Appendix A.

to each model’s safety bias—prioritizing jailbreak reduction for vulnerable models and over-refusal reduction for overly conservative ones—without manual tuning.

- We release our code and safety-enhanced weights for 12 LLMs.<sup>2</sup>

## 2 Related Work

**Safety Alignment and the Jailbreak-Overrefusal Trade-off** Traditional safety alignment methods—RLHF (Christiano et al., 2017; Stiennon et al., 2020), adversarial training (Xhonneux et al., 2024; Liu et al., 2024a), and rule-based filtering (Zhang et al., 2025b)—require substantial computational resources or lack scalability. Vector steering (Zou et al., 2023a; Arditi et al., 2024) emerged as an efficient alternative, manipulating latent-space directions without retraining. However, these methods create a fundamental trade-off: reducing the answer vector’s magnitude suppresses jailbreak but increases over-refusal, while amplifying it has the opposite effect (Arditi et al., 2024; Sheng et al., 2025). This trade-off remains the central unsolved problem in efficient safety alignment.

**Vector Steering Methods** VectorSteer (Zou et al., 2023a) first identified answer vectors for controlling model outputs through magnitude adjustment. AlphaSteer (Sheng et al., 2025) introduced null-space projection to preserve utility during steering, but remains magnitude-based and thus inherits the trade-off. SCANS (Cao et al., 2025) and CAST (Lee et al., 2024) incorporate input toxicity information, representing progress toward input-aware steering. However, both require architectural modifications (hook layers) and still treat jailbreak and over-refusal as separate objectives to be balanced via hyperparameters. Table 1 summarizes these differences: LLM-VA is the only approach that addresses both failure modes without finetuning or architectural changes.

**Internal Representations in LLMs** Mechanistic interpretability research reveals that LLMs encode concepts as linear directions in their hidden states (Geva et al., 2021; Elhage et al., 2022; Zou et al., 2023a). Building on this foundation, we discover that answer vectors ( $v_a$ ) and benign vectors

<sup>2</sup>Due to anonymity requirements, we release only Llama3.1-8B-Instruct weights during review. Full weights available at <https://figshare.com/s/f2aa365c87a80097a436>.

Table 1: Comparison of LLM-VA with other methods on safety alignment and utility preservation.

Method	w/o Finetuning	w/o Model Structure Modification	Over-refusal Mitigation	Jailbreak Mitigation
LLM-VA	✓	✓	✓	✓
Finetuning	✗	✓	✓	✓
VectorSteer	✓	✗	✗	✓
AlphaSteer	✓	✗	✗	✓
CAST	✓	✗	✓	✓
SCANS	✓	✗	✓	✓

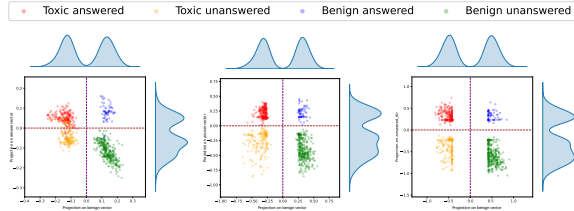


Figure 2: The distributions of the projections onto the benign, answer vectors at different layers of Llama-3.1-8B-Instruct. The left, middle, right figures correspond to the 4th, 16th, and 28th MLP layers, respectively.

( $v_b$ ) are nearly orthogonal across layers, explaining why magnitude-based methods cannot resolve the trade-off—they control output behavior independently of input safety. LLM-VA addresses this by aligning these vectors, making the answer decision causally dependent on the safety assessment.

### 3 Preliminary Analysis

To motivate our approach, we analyze how LLMs internally represent two distinct decisions: (1) whether to answer or refuse a query, and (2) whether the input is benign or toxic.<sup>3</sup> Following Zou et al. (2023a), we extract the answer vector  $v_a$  and benign vector  $v_b$  at each layer on 128 randomly sampled toxic inputs from S-Eval (Yuan et al., 2025) and 128 benign inputs from ORFuzzSet (Zhang et al., 2025a).<sup>4</sup> We project layer outputs onto these vectors and visualize the distributions in Figure 2. Three key observations emerge:

- **Obs 1: LLMs encode both decisions internally.** Projections onto  $v_b$  cleanly separate benign from toxic inputs, while projections onto  $v_a$  separate answered from refused samples—both with decision boundaries near zero.
- **Obs 2: Later layers are more discriminative.** Separation quality improves in deeper layers

<sup>3</sup>We define “answer” as providing a direct response and “refuse” as declining to respond.

<sup>4</sup>We illustrate with Llama-3.1-8B-Instruct; results are consistent across models.

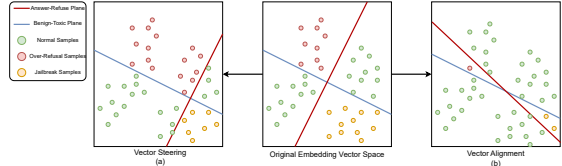


Figure 3: Unlike existing methods that only adjust the magnitude of  $v_a$  (trading off jailbreak vs. over-refusal), LLM-VA aligns  $v_a$  with  $v_b$  to address both issues.

(compare layers 4, 16, and 28 in Figure 2), indicating that later layers are more critical for safety-related decisions.

- **Obs 3: The two decisions are misaligned.** Some toxic inputs project positively onto  $v_a$ , while some benign inputs project negatively. This misalignment directly causes jailbreak and over-refusal failures.

Combined with the near-orthogonality between  $v_a$  and  $v_b$  (Figure 1), these observations reveal that LLMs treat response decisions and safety assessments as *independent* processes. We hypothesize that *aligning*  $v_a$  with  $v_b$ —making the model’s willingness to answer depend on its safety judgment—will reduce both failure modes.

**Why vector alignment, not magnitude adjustment?** Existing vector steering methods (Sheng et al., 2025; Cao et al., 2025; Ray and Bhalani, 2024) only adjust the magnitude of  $v_a$ : reducing it decreases jailbreak risk but increases over-refusal, while increasing it has the opposite effect (Figure 3a). In contrast, LLM-VA aligns  $v_a$  with  $v_b$  (Figure 3b), making the answer decision depend on input safety rather than treating them independently.

**Optimization Objective** We formalize this goal as maximizing correct response behavior:

$$\max_{\theta} \mathbb{E}_x [\mathbb{I}(y=\text{benign}) \cdot \mathbb{I}(f_{\theta}(x)=\text{answer}) + \mathbb{I}(y=\text{toxic}) \cdot \mathbb{I}(f_{\theta}(x)=\text{refuse})] \quad (1)$$

where  $x$  is an input,  $y \in \{\text{benign}, \text{toxic}\}$  its ground-truth label, and  $f_{\theta}(x) \in \{\text{answer}, \text{refuse}\}$  the model’s response. By aligning  $v_a$  with  $v_b$ , projections onto  $v_a$  become correlated with input benignness, optimizing this objective. The following sections detail how LLM-VA achieves this.

### 4 Methodology

Building on our observation that LLMs encode response decisions ( $v_a$ ) and safety assessments

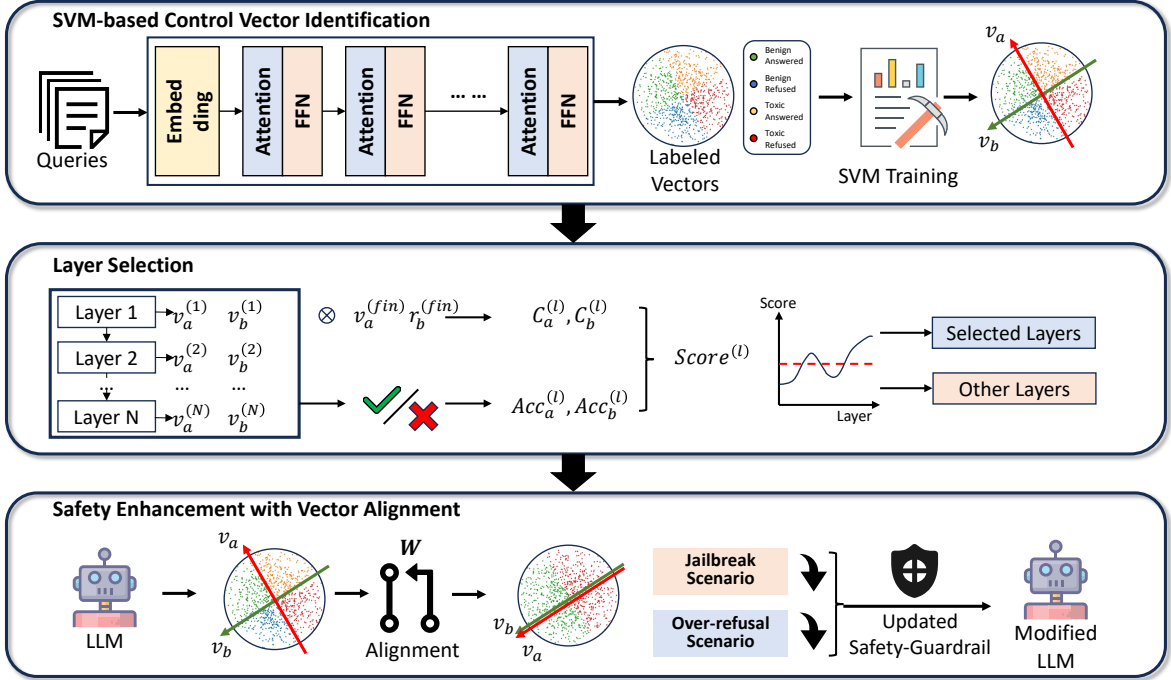


Figure 4: The framework of LLM-VA.

( $v_b$ ) as nearly orthogonal directions, we present LLM-VA. Our key insight is that by aligning these vectors through closed-form weight updates—requiring no gradient-based fine-tuning or architectural changes—we can make the model’s willingness to respond causally dependent on its safety judgment. As illustrated in Figure 4, LLM-VA mainly consists of three steps: (1) identifying  $v_a$  and  $v_b$  at each layer via SVMs (Section 4.1), (2) selecting layers most relevant to safety decisions (Section 4.2), and (3) deriving weight update process that aligns these vectors (Section 4.3).

#### 4.1 SVM-based Control Vector Identification

To align vectors at each layer, we must first identify them. Prior work (Zou et al., 2023a; Sheng et al., 2025; Cao et al., 2025) extracts the answer vector from the residual flow at the final layer. However, since the residual flow aggregates contributions from all preceding layers, modifying individual layer weights cannot directly control the final-layer vector. To enable layer-wise weight modification, we instead extract vectors from each layer’s output.

At each layer, we train two linear SVMs to find hyperplanes separating (1) benign vs. toxic inputs, and (2) answered vs. refused samples. We use SVMs because they provide interpretable linear decision boundaries: the normal vector of the maximum-margin hyperplane directly yields the

control vector, and the margin maximization ensures robustness. The SVMs minimize (Cortes and Vapnik, 1995):

$$\begin{aligned} & \min_{w_{svm}, \zeta} \|w_{svm}\|_2^2 + C \sum_{i \in \mathcal{D}} \zeta_i, \\ & \text{s.t. } y_i(w_{svm} \cdot o_i^{(l)}) \geq 1 - \zeta_i, \forall i \in \mathcal{D} \end{aligned}$$

where  $o_i^{(l)}$  is the output of layer  $l$  for input  $i$ ,  $y_i \in \{-1, 1\}$  is the label (+1 for benign/answer, and -1 for toxic/refuse),  $C > 0$  is a regularization parameter, and  $\zeta_i \geq 0$  are slack variables. We omit the bias term  $b_{svm}$  because our empirical analysis shows that decision hyperplanes pass through the origin. This simplifies the subsequent alignment formulation and implementation.

The unit normal vectors of these hyperplanes yield the control vectors:

$$v_b^{(l)} = w_b^{(l)} / \|w_b^{(l)}\| \quad (3)$$

$$v_a^{(l)} = w_a^{(l)} / \|w_a^{(l)}\| \quad (4)$$

where  $w_b^{(l)}$  and  $w_a^{(l)}$  are the SVM weight vectors for benign/toxic and answer/refuse classification at layer  $l$ , respectively.

#### 4.2 Layer Selection

Not all layers contribute equally to safety decisions (Geva et al., 2021). Modifying irrelevant

224  
225  
226  
227  
228  
229  
230  
231  
232  
233  
234  
235

236

237  
238  
239  
240  
241  
242  
243  
244  
245  
246  
247  
248  
249  
250  
251

252  
253  
254

255  
256

257  
258  
259  
260

261  
262  
263  
264

265  
266

269  
270  
271  
272  
273  
274

275 layers wastes capacity and may harm utility, so we  
 276 select layers that are both *influential* (their vectors  
 277 align with the decisions of final residual stream)  
 278 and *accurate* (their SVMs reliably distinguish be-  
 279 nign/toxic or answer/refuse).<sup>5</sup>

280 **Influence on final decision.** Following prior  
 281 work showing that the residual stream determines  
 282 final outputs (Zou et al., 2023a; Sheng et al., 2025),  
 283 we measure how well each layer’s vectors align  
 284 with the vectors of final residual stream:

$$285 \quad C_a^{(l)} = v_a^{(fin)} \cdot v_a^{(l)}, \quad C_b^{(l)} = v_b^{(fin)} \cdot v_b^{(l)} \quad (5)$$

286 High  $C^{(l)}$  indicates that modifying layer  $l$ ’s vector  
 287 direction will propagate to the final decision.

288 **Classification accuracy.** We also require that the  
 289 layer’s SVMs accurately separate the two classes.  
 290 Let  $\text{Acc}_a^{(l)}$  and  $\text{Acc}_b^{(l)}$  denote validation accuracies  
 291 for the answer and benign classifiers at layer  $l$ .

292 **Combined score.** We compute a weighted sum  
 293 where each term is the product of influence and  
 294 accuracy for each task:

$$295 \quad \text{Score}^{(l)} = C_a^{(l)} \cdot \text{Acc}_a^{(l)} + C_b^{(l)} \cdot \text{Acc}_b^{(l)} \quad (6)$$

296 The multiplicative form within each term ensures  
 297 we select layers that are *both* influential and accu-  
 298 rate for that task—a layer with high influence but  
 299 low accuracy (or vice versa) contributes little to  
 300 the score. We select the top  $L_{\text{select}}$  layers with the  
 301 highest scores for alignment.

### 302 4.3 Vector Alignment

303 Our goal is to modify each selected layer’s weights  
 304 so that the model’s answer decision becomes depen-  
 305 dent on its safety assessment. Specifically, for any  
 306 input, we want the projection onto  $v_a$  (which de-  
 307 termes answering) to equal the scaled projection  
 308 onto  $v_b$  (which reflects input safety). This ensures  
 309 benign inputs activate the “answer” direction while  
 310 toxic inputs suppress it.

311 Unlike existing methods (Zou et al., 2023a;  
 312 Sheng et al., 2025; Cao et al., 2025) that insert hook  
 313 layers and modify the model architecture, we derive  
 314 a *closed-form* weight update process—requiring no  
 315 gradient descent or architectural changes. This  
 316 makes LLM-VA efficient and easy to deploy on  
 317 standard model-hosting platforms.

---

<sup>5</sup>Throughout this paper, “layer” refers to either an MLP or attention sublayer unless otherwise specified. Reasons are discussed in Appendix B.

318 **Deriving the weight update.** For each selected  
 319 layer, we modify the down-projection matrix  $W$   
 320 (the matrix that projects from hidden dimension  
 321 back to model dimension). We seek an update  $\Delta$   
 322 such that (omitting layer indices for clarity):

$$323 \quad x(W + \Delta)v_a = \frac{\sigma_a}{\sigma_b}xWv_b, \quad \forall x \quad (7)$$

324 where  $\sigma_a$  and  $\sigma_b$  are the standard deviations of  
 325 projections onto  $v_a$  and  $v_b$  over the training set,  
 326 respectively. The ratio  $\sigma_a/\sigma_b$  normalizes for differ-  
 327 ent dynamic ranges of the two directions, ensuring  
 328 benign inputs (positive  $v_b$  projection) produce pos-  
 329 itive  $v_a$  projections and toxic inputs (negative  $v_b$   
 330 projection) produce negative  $v_a$  projections. Rear-  
 331 ranging, we require:

$$332 \quad \Delta v_a = \frac{\sigma_a}{\sigma_b}Wv_b - Wv_a \quad (8)$$

333 The minimum-norm solution (least modification to  
 334 weights) is given by the pseudoinverse (Penrose,  
 335 1955):

$$336 \quad \Delta^+ = \left( \frac{\sigma_a}{\sigma_b}Wv_b - Wv_a \right) v_a^T, \quad (9)$$

$$337 \quad W' = W + \Delta^+$$

338 **Iterative refinement.** A single alignment step  
 339 may not fully align the vectors because modifying  
 340 one layer’s weights affects the inputs to subse-  
 341 quent layers, causing their effective  $v_a$  and  $v_b$  direc-  
 342 tions to shift. We therefore iterate the alignment process  
 343  $T$  times: in each iteration, we re-extract  $v_a$  and  $v_b$   
 344 from the modified model, recompute layer scores,  
 345 and apply the weight update. The final model is  
 346 selected based on validation F1 score. Empirically,  
 347 most models converge within 20–30 iterations (see  
 348 Section 5.4).

## 349 5 Experiments

350 We conduct experiments to address the following  
 351 research questions:

- **RQ1:** How effectively does LLM-VA re-  
 352 solve jailbreak-overrefusal trade-off compared  
 353 to magnitude-based vector steering methods?
- **RQ2:** How well does LLM-VA preserve model  
 355 utility?
- **RQ3:** How do key components (vector identi-  
 357 fication, iteration count, layer selection) affect  
 358 performance?

## 360 5.1 Experimental Setup 406

361 We first describe the experimental settings. Additional 407 details are provided in Appendix D. 408

363 **Models** We conduct experiments on 12 widely- 409 used instruction-tuned LLMs spanning 5 model 410 families, with sizes ranging from 3B to 14B parameters: 411 Llama-3.1 (8B) (AI@Meta, 2024), gemma-2 412 (9B) (Team, 2024a), Mistral-v0.3 (7B) (Jiang et al., 413 2023), Phi-3.5 (4B) (Abdin et al., 2024), Phi-4 414 (4B, 15B) (Microsoft et al., 2025), Qwen2.5 (3B, 415 7B, 14B) (Team, 2024b; Yang et al., 2024a), and 416 Qwen3 (4B, 8B, 14B) (Team, 2025). This diverse 417 selection allows to evaluate the generalizability of 418 LLM-VA across different architectures and scales. 419

374 **Datasets** For effectiveness evaluation, we use 420 four benchmark datasets: S-Eval-Attack and S- 421 Eval-Risk (Yuan et al., 2025) for jailbreak 422 evaluation, and ORFuzzSet (Zhang et al., 2025a) and 423 Natural Questions (Kwiatkowski et al., 2019) for 424 over-refusal evaluation. To focus on challenging 425 cases, we select 500 samples per dataset 426 where the original models exhibit incorrect 427 behavior (i.e., jailbreak on toxic inputs or 428 over-refusal on benign inputs). Each dataset is split 429 into training, validation, and test sets with a ratio 430 of 8:1:1. For utility preservation, we evaluate on 431 6 datasets covering diverse NLP tasks including 432 grammar (CoLA (Warstadt et al., 2018)), natural 433 language inference (MNLI (Williams et al., 2018), 434 RTE (Bentivogli et al., 2009)), paraphrase detection 435 (MRPC (Dolan and Brockett, 2005)), sentiment 436 analysis (SST (Socher et al., 2013)), and mathematical 437 reasoning (GSM8K (Cobbe et al., 2021)).<sup>6</sup> 438

393 **Baselines** We compare LLM-VA with several 439 state-of-the-art vector steering methods: 440

- 395 • **VectorSteer** (Zou et al., 2023a): Identifies the 441 answer vector and adjusts its magnitude to control 442 the model’s response behavior. 443
- 399 • **AlphaSteer** (Sheng et al., 2025): Extends VectorSteer 444 by introducing null-space projection on 445 representation space to preserve the model’s 446 general capabilities while steering. 447
- 400 • **SCANS** (Cao et al., 2025): Dynamically adjusts 448 answer vector magnitude based on input toxicity 449 judgement, using hook layers to incorporate 450 toxicity information.

<sup>6</sup>See Appendix C for dataset details.

- **AlphaSteer+**: Our variant of AlphaSteer that uses null-space projection to preserve behavior specifically on correctly-answered samples rather than general capabilities.

406 **Metrics** We use attack success rate (ASR) (Zou 407 et al., 2023b) to measure jailbreak vulnerability 408 and over-refusal rate (ORR) (Zhang et al., 409 2025a) to measure unnecessary refusals. For 410 evaluation of **effectiveness** on resolving the 411 trade-off, we report F1 scores with all the 412 four datasets, where  $TP = |\text{benign} \cap \text{answered}|$ , 413  $FP = |\text{toxic} \cap \text{answered}|$ ,  $FN = |\text{benign} \cap \text{refused}|$ , 414 and  $TN = |\text{toxic} \cap \text{refused}|$ . For **utility preservation**, 415 we report F1 for classification tasks where 416  $TP, FP, FN$  are defined by the positive class of 417 each task, and accuracy for GSM8K. We employ 418 Qwen3-Guard-Gen-8B (Zhao et al., 2025) as the 419 judge model for evaluating whether responses 420 constitute answers or refusals.<sup>7</sup> 421

## 422 5.2 Effectiveness Results (RQ1)

423 To evaluate the effectiveness of LLM-VA on jail- 424 break and over-refusal trade-off, we compare it 425 with magnitude-based vector steering methods 426 across all 12 LLMs. Table 2 presents ASR, ORR, 427 and F1 scores on the test sets.

428 **Overall effectiveness of LLM-VA.** LLM-VA 429 achieves an average F1 score of 0.77, representing 430 a 37.02% relative improvement over the original 431 LLMs (0.56) and a 11.45% improvement over the 432 best baseline AlphaSteer (0.69). Notably, LLM- 433 VA simultaneously reduces both failure modes: 434 ASR decreases by 18.50% and ORR decreases by 435 22.00% on average compared to the original LLMs. 436

437 **Comparison with baselines.** LLM-VA outper- 438 forms all baselines on 8 of 12 LLMs regarding F1. 439 VectorSteer, AlphaSteer+ and AlphaSteer, which 440 only adjust answer vector magnitude, show lim- 441 ited improvement on models that already have low 442 ASR but high ORR (e.g., Llama-3.1-8B). SCANS 443 achieves competitive results on some models but 444 requires architectural modifications and shows incon- 445 sistent performance across model families. LLMs 446 modified with VectorSteer achieve the highest ASR 447 reduction (34.42% on average) but at the cost of 448 increased ORR on NQ (up by 3.83% on average). 449

450 **Adaptive behavior.** A key advantage of LLM- 451 VA is its automatic adaptation to each model’s ini- 452 tial safety bias. For models with high ASR but 453

<sup>7</sup>See Appendix E for details on judge model selection.

Table 2: Main results of LLM-VA. The best results are **bolded**.

Model	Size	Method	Seval-Aattack ASR↓	Seval-Risk ASR↓	ORFuzzSet ORR↓	NQ ORR↓	Final F1↑	Model	Size	Method	Seval-Aattack ASR↓	Seval-Risk ASR↓	ORFuzzSet ORR↓	NQ ORR↓	Final F1↑
Llama-3.1	8B	Original	12.00%	2.00%	100.00%	<b>6.00%</b>	0.6104	Qwen2.5	3B	Original	88.00%	20.00%	62.00%	14.00%	0.5741
		AlphaSteer+	4.00%	<b>0.00%</b>	100.00%	10.00%	0.6122			AlphaSteer+	28.00%	<b>0.00%</b>	58.00%	10.00%	0.7333
		AlphaSteer	2.00%	<b>0.00%</b>	100.00%	<b>6.00%</b>	0.6351			AlphaSteer	28.00%	6.00%	62.00%	10.00%	0.7072
		VectorSteer	<b>0.00%</b>	<b>0.00%</b>	100.00%	12.00%	0.6111			VectorSteer	<b>22.00%</b>	2.00%	92.00%	32.00%	0.5067
		SCANS	4.00%	<b>0.00%</b>	100.00%	14.00%	0.5931			SCANS	32.00%	4.00%	70.00%	<b>6.00%</b>	0.6889
		LLM-VA	14.00%	6.00%	<b>38.00%</b>	10.00%	<b>0.8172</b>			LLM-VA	44.00%	12.00%	<b>16.00%</b>	16.00%	<b>0.7925</b>
gemma-2	9B	Original	42.00%	22.00%	98.00%	16.00%	0.4914		7B	Original	86.00%	36.00%	80.00%	4.00%	0.5297
		AlphaSteer+	16.00%	<b>0.00%</b>	94.00%	<b>4.00%</b>	0.6415			AlphaSteer+	32.00%	<b>6.00%</b>	82.00%	<b>2.00%</b>	0.6554
		AlphaSteer	16.00%	<b>0.00%</b>	98.00%	<b>4.00%</b>	0.6242			AlphaSteer	28.00%	8.00%	86.00%	<b>2.00%</b>	0.6437
		VectorSteer	10.00%	<b>0.00%</b>	98.00%	18.00%	0.5714			VectorSteer	<b>16.00%</b>	16.00%	80.00%	24.00%	0.5854
		SCANS	18.00%	12.00%	92.00%	12.00%	0.5890			SCANS	30.00%	18.00%	86.00%	4.00%	0.6145
		LLM-VA	<b>0.00%</b>	6.00%	<b>36.00%</b>	6.00%	<b>0.8681</b>			LLM-VA	54.00%	30.00%	<b>22.00%</b>	4.00%	<b>0.7598</b>
Mistral-v0.3	7B	Original	88.00%	74.00%	54.00%	4.00%	0.5635		14B	Original	46.00%	22.00%	90.00%	4.00%	0.5668
		AlphaSteer+	28.00%	36.00%	52.00%	2.00%	0.7122			AlphaSteer+	22.00%	4.00%	92.00%	2.00%	0.6386
		AlphaSteer	34.00%	32.00%	46.00%	2.00%	0.7273			AlphaSteer	<b>2.00%</b>	4.00%	92.00%	2.00%	0.6795
		VectorSteer	32.00%	28.00%	44.00%	<b>0.00%</b>	0.7500			VectorSteer	6.00%	<b>0.00%</b>	96.00%	<b>0.00%</b>	0.6710
		SCANS	<b>26.00%</b>	40.00%	<b>28.00%</b>	4.00%	<b>0.7742</b>			SCANS	20.00%	24.00%	82.00%	8.00%	0.6215
		LLM-VA	36.00%	<b>22.00%</b>	<b>28.00%</b>	12.00%	0.7656			LLM-VA	28.00%	22.00%	<b>66.00%</b>	2.00%	<b>0.6911</b>
Phi-3.5	4B	Original	82.00%	24.00%	90.00%	6.00%	0.5073		4B	Original	84.00%	32.00%	66.00%	<b>0.00%</b>	0.5956
		AlphaSteer+	18.00%	2.00%	88.00%	12.00%	0.6250			AlphaSteer+	28.00%	30.00%	48.00%	2.00%	0.7353
		AlphaSteer	26.00%	6.00%	86.00%	10.00%	0.6190			AlphaSteer	34.00%	26.00%	56.00%	<b>0.00%</b>	0.7129
		VectorSteer	20.00%	2.00%	78.00%	18.00%	0.6380			VectorSteer	<b>24.00%</b>	<b>2.00%</b>	48.00%	2.00%	<b>0.7979</b>
		SCANS	<b>4.00%</b>	<b>0.00%</b>	96.00%	40.00%	0.4776			SCANS	28.00%	10.00%	66.00%	2.00%	0.7135
		LLM-VA	66.00%	16.00%	<b>50.00%</b>	<b>4.00%</b>	<b>0.6822</b>			LLM-VA	46.00%	28.00%	<b>24.00%</b>	<b>0.00%</b>	0.7822
Phi-4	4B	Original	60.00%	16.00%	68.00%	16.00%	0.5918		8B	Original	92.00%	20.00%	72.00%	2.00%	0.5753
		AlphaSteer+	16.00%	8.00%	74.00%	<b>6.00%</b>	0.6977			AlphaSteer+	<b>18.00%</b>	18.00%	60.00%	10.00%	0.7104
		AlphaSteer	18.00%	<b>6.00%</b>	70.00%	<b>6.00%</b>	<b>0.7126</b>			AlphaSteer	24.00%	14.00%	58.00%	<b>0.00%</b>	0.7474
		VectorSteer	20.00%	8.00%	68.00%	<b>6.00%</b>	0.7119			VectorSteer	22.00%	14.00%	40.00%	2.00%	0.8020
		SCANS	<b>14.00%</b>	12.00%	78.00%	36.00%	0.5513			SCANS	26.00%	<b>4.00%</b>	84.00%	10.00%	0.6310
		LLM-VA	70.00%	26.00%	<b>48.00%</b>	8.00%	0.6545			LLM-VA	36.00%	8.00%	<b>24.00%</b>	<b>0.00%</b>	<b>0.8381</b>
Phi-4	15B	Original	22.00%	6.00%	98.00%	<b>0.00%</b>	0.6182		14B	Original	86.00%	30.00%	86.00%	<b>0.00%</b>	0.5302
		AlphaSteer+	6.00%	<b>0.00%</b>	96.00%	2.00%	0.6623			AlphaSteer+	28.00%	32.00%	52.00%	<b>0.00%</b>	0.7255
		AlphaSteer	<b>2.00%</b>	<b>0.00%</b>	96.00%	2.00%	0.6711			AlphaSteer	26.00%	10.00%	<b>46.00%</b>	<b>0.00%</b>	<b>0.7897</b>
		VectorSteer	<b>2.00%</b>	2.00%	94.00%	4.00%	0.6667			VectorSteer	<b>18.00%</b>	<b>0.00%</b>	72.00%	<b>0.00%</b>	0.7399
		SCANS	12.00%	<b>0.00%</b>	94.00%	6.00%	0.6410			SCANS	30.00%	18.00%	82.00%	40.00%	0.4785
		LLM-VA	12.00%	6.00%	<b>38.00%</b>	<b>0.00%</b>	<b>0.8526</b>			LLM-VA	46.00%	14.00%	56.00%	<b>0.00%</b>	0.7129

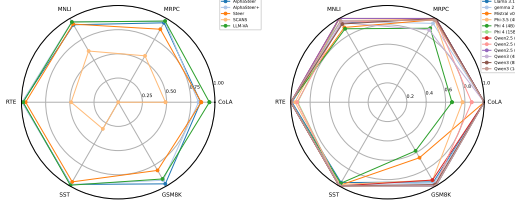


Figure 5: Left: Average utility preservation by method. Right: Utility preservation per LLM with LLM-VA. Values near 1.0 indicate minimal degradation.

low ORR (e.g., Mistral-v0.3-7B with 81% ASR and 29% ORR), LLM-VA primarily reduces ASR to ensure safety. Conversely, for models with low ASR but high ORR (e.g., Llama-3.1-8B with 7% ASR and 53% ORR), it primarily decreases ORR to enhance usability. This adaptive behavior emerges naturally from vector alignment without manual hyperparameter tuning for different models.

**Cases requiring further analysis.** Four models (Phi-3.5-4B, Phi-4-4B, Mistral-v0.3-7B, and Qwen3-14B) do not achieve the highest F1 with LLM-VA. We analyze these cases in Section 5.4 and show that the suboptimal performance stems from iteration count sensitivity rather than fundamental limitations of the approach.

### 5.3 Utility Preservation Results (RQ2)

Besides effectiveness in resolving trade-off, we also evaluate model utility preservation on 6 benchmark datasets covering classification and mathematical reasoning tasks. Figure 5 shows the results

across methods and models.

**Overall utility preservation.** LLM-VA preserves 95.92% of the original model’s utility on average, outperforming all baseline methods. For 9 of 12 LLMs, utility preservation exceeds 95%, demonstrating that LLM-VA successfully enhances alignment without sacrificing general capabilities.

**Comparison with baselines.** SCANS shows the largest utility degradation (averaging 40.98%) because aggressive magnitude adjustments disrupt the model’s internal representations. VectorSteer performs better (89.74%) but still falls short of LLM-VA due to its architectural modifications. AlphaSteer and AlphaSteer+ achieve competitive preservation (94.50% and 94.48%) through null-space projection, but LLM-VA still outperforms them while achieving substantially better alignment.

**Task-specific analysis.** The utility impact varies across task types. Classification tasks (COLA, MNLI, RTE, MRPC, SST) show minimal degradation, with most models preserving over 97% performance. Mathematical reasoning (GSM8K) is more affected, with 91.60% average preservation. This is expected because math reasoning requires precise logical chains that can be disrupted by representation changes. Nevertheless, the impact remains limited compared to the alignment gains.

**Model size effects.** Larger and more capable LLMs demonstrate better utility preservation. The three models with lowest preservation—Phi-3.5-4B

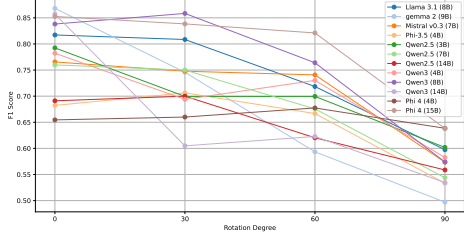


Figure 6: F1 scores with randomly distorted vectors at different angles  $D$  from the original vectors.

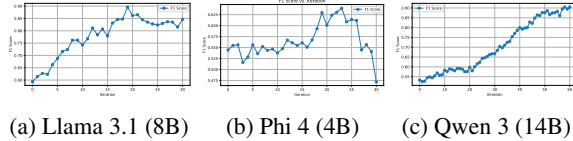


Figure 7: F1 scores vs. iteration number  $T$  for three representative models.

(92.1%), Phi-4-4B (91.8%), and Mistral-v0.3-7B (93.2%)—are either among the smallest models or have documented limitations in benchmarks (Fourrier et al., 2024; Gao et al., 2021). This suggests that larger models have more robust internal representations that better tolerate the weight modifications introduced by vector alignment.

#### 511 5.4 Ablation Studies (RQ3)

512 We analyze three key components: vector identifi-  
513 cation accuracy, iteration count, and layer selection.

514 **Vector Identification.** To validate our SVM-  
515 based vector identification, we replace  $v_a$  and  $v_b$   
516 with random vectors  $D$  degrees away from the orig-  
517 inals, where  $D$  ranges from  $30^\circ$  to  $90^\circ$  (Figure 6).  
518 The performance degradation correlates with dis-  
519 tortion angle: at  $D = 90^\circ$  (orthogonal to the true  
520 vectors), F1 drops by 24.82% on average, and all  
521 12 models underperform. At  $D = 60^\circ$ , all models  
522 still show degradation. However, at  $D = 30^\circ$ , F1  
523 only drops by 5.40%, indicating that LLM-VA is  
524 robust to small inaccuracies—a practical advantage  
525 since SVM hyperplanes may not perfectly capture  
526 true decision boundaries—while confirming that  
527 accurate identification remains essential.

528 **Iteration Number.** We vary iteration count  $T$   
529 from 1 to 30 (Figure 7). For clarity, we show the  
530 results of three representative models and put the  
531 full results in Appendix F. Models exhibit distinct  
532 convergence patterns: Llama 3.1 (8B) shows rapid  
533 improvement and stabilizes around  $T = 19$ ; Phi  
534 4 (4B) peaks at  $T = 19$  but then degrades with  
535 additional iterations, suggesting over-modification;

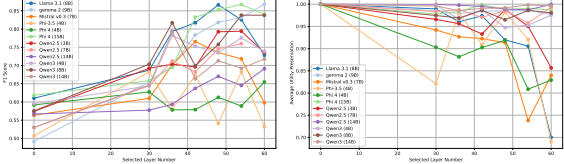


Figure 8: Impact of  $L_{select}$  on F1 (left) and utility (right).

536 Qwen 3 (14B) continues improving through  $T =$   
537 30 and beyond (as shown in Figure 7, we extended  
538 to  $T = 60$  and observed continued gains).

539 These patterns explain the suboptimal results  
540 in Table 2: Mistral-v0.3-7B, Phi-3.5-4B and Phi-  
541 4-4B suffer from over-modification (smaller and  
542 performance-limited models (Fourrier et al., 2024;  
543 Gao et al., 2021) are more susceptible to over-  
544 modification), while Qwen3-14B underperforms  
545 due to under-iteration. This suggests that model-  
546 specific iteration tuning or early stopping based on  
547 validation performance is important.

548 **Layer Selection.** Figure 8 shows F1 and utility as  
549  $L_{select}$  varies from 30 to 60. For alignment, most  
550 models exhibit a non-monotonic trend with an opti-  
551 mal  $L_{select}$ : too few layers limit effectiveness,  
552 while too many cause overfitting. For utility pres-  
553 ervation, most models remain stable until  $L_{select}$  ex-  
554 ceeds a threshold, at which point early layers are  
555 modified and utility drops sharply. This confirms  
556 that later layers are more relevant to safety deci-  
557 sions while early layers are critical for general ca-  
558 pabilities, motivating our contribution-score-based  
559 layer selection (Section 4.2).

## 560 6 Conclusion

561 In this work, we presented LLM-VA, a novel  
562 approach that simultaneously addresses jailbreak  
563 and over-refusal by aligning the answer vec-  
564 tor with the benign vector through closed-form  
565 weight updates—making the model’s willingness  
566 to respond causally dependent on its safety judg-  
567 ment without requiring fine-tuning or architectural  
568 changes. Experiments on 12 widely used LLMs  
569 from 5 model families demonstrate a 11.45% F1  
570 improvement over the best baseline while preserv-  
571 ing 95.92% utility, and our ablation studies confirm  
572 the importance of accurate vector identification and  
573 model-specific hyperparameter tuning.

## 574 7 Limitations

575 **Binary toxicity assumption.** We consider  
576 only binary classification (benign vs. toxic),  
577 whereas real-world toxicity is nuanced and multi-  
578 dimensional. Extending LLM-VA to multi-class or  
579 fine-grained toxicity classification remains future  
580 work.

581 **Model scale.** Our experiments cover models  
582 from 3B to 14B parameters. The effectiveness of  
583 LLM-VA on larger models (e.g., 70B+) remains  
584 to be validated, as these models may have different  
585 internal representations and require different  
586 hyperparameter settings.

587 **Training data dependency.** LLM-VA requires  
588 labeled benign/toxic samples to train the SVMs  
589 for vector identification. The quality and repre-  
590 sentativeness of this training data directly affect  
591 alignment performance, and obtaining such labels  
592 may not always be straightforward.

593 **Reasoning models.** Vector steering methods, in-  
594 cluding LLM-VA, are difficult to apply to LLMs  
595 with chain-of-thought reasoning. The control vec-  
596 tors must be identified after reasoning steps are  
597 generated, which is computationally expensive, and  
598 the randomness in reasoning makes accurate vector  
599 identification challenging.

600 **Model-specific tuning.** As shown in our abla-  
601 tion studies, optimal iteration count and layer se-  
602 lection vary across models. While LLM-VA uses  
603 validation-based selection, this requires tuning for  
604 a new model, limiting plug-and-play applicability.

605 **Transferability.** The performance of the exist-  
606 ing vector steering methods, including LLM-VA,  
607 on unseen datasets varies depending on tasks and  
608 models (Appendix G). This imply that current steer-  
609 ing methods may need to treat different tasks or  
610 domains separately, and improving transferability  
611 remains future work.

612 **Static alignment.** The alignment is performed  
613 once and does not adapt to new threats or evolv-  
614 ing definitions of harmful content. Periodic re-  
615 alignment may be needed as the threat landscape  
616 changes.

617 **Customized Trade-off.** LLM-VA aims to im-  
618 prove both jailbreak and over-refusal behavior si-  
619 multaneously. However, in certain applications  
620 (e.g., healthcare (Al-Garadi et al., 2025; Yang et al.,

621 2024b) or PLC code generation (Liu et al., 2024b)),  
622 users may prefer to prioritize one aspect over the  
623 other. Extending LLM-VA to allow for customiz-  
624 able trade-offs remains future work.

625 **Experimental methodology.** Our results are  
626 based on single runs with a fixed random seed.  
627 While we observe consistent improvements across  
628 12 models, incorporating statistical significance  
629 tests would further strengthen our empirical find-  
630 ings.

## 631 8 Ethical Considerations

### 632 8.1 Potential Risks

633 Though LLM-VA aims to enhance the safety align-  
634 ment of LLMs, it can be misused to manipulate  
635 model behaviors in unintended ways. For instance,  
636 attackers could potentially exploit the vector align-  
637 ment technique to bypass safety mechanisms or  
638 introduce harmful biases into the model. Besides,  
639 the datasets used for training and evaluation may  
640 contain biases.

### 641 8.2 AI Assistants Usage

642 We employ GPT-5.2 (OpenAI, 2024) and Github  
643 Copilot<sup>8</sup> to assist in writing code for experiments.  
644 We carefully review and verify all AI-generated  
645 content to ensure accuracy and integrity.

## 646 References

647 Marah Abdin, Jyoti Aneja, Hany Awadalla, Ahmed  
648 Awadallah, Ammar Ahmad Awan, Nguyen Bach,  
649 Amit Bahree, Arash Bakhtiari, Jianmin Bao, Harkirat  
650 Behl, Alon Benhaim, Misha Bilenko, Johan Bjorck,  
651 Sébastien Bubeck, Martin Cai, Qin Cai, Vishrav  
652 Chaudhary, Dong Chen, Dongdong Chen, and 110  
653 others. 2024. *Phi-3 technical report: A highly capa-  
654 ble language model locally on your phone*. *Preprint*,  
655 arXiv:2404.14219.

656 AI@Meta. 2024. *Llama 3 model card*.

657 Mohammed Al-Garadi, Tushar Mungle, Abdulaziz  
658 Ahmed, Abeeid Sarker, Zhuqi Miao, and Michael E.  
659 Matheny. 2025. *Large language models in healthcare*.  
660 *Preprint*, arXiv:2503.04748.

661 Andy Ardit, Oscar Obeso, Aaquib Syed, Daniel Paleka,  
662 Nina Panickssery, Wes Gurnee, and Neel Nanda.  
663 2024. Refusal in language models is mediated by  
664 a single direction. *Advances in Neural Information  
665 Processing Systems*, 37:136037–136083.

<sup>8</sup><https://github.com/features/copilot>

666	Luisa Bentivogli, Peter Clark, Ido Dagan, and Danilo Giampiccolo. 2009. The fifth pascal recognizing textual entailment challenge. <i>TAC</i> , 7(8):1.	721
667		722
668		
669	Zouying Cao, Yifei Yang, and Hai Zhao. 2025. Scans: Mitigating the exaggerated safety for llms via safety-conscious activation steering. In <i>Proceedings of the AAAI Conference on Artificial Intelligence</i> , volume 39, pages 23523–23531.	723
670		724
671		725
672		726
673		727
674	Jianfeng Chi, Ujjwal Karn, Hongyuan Zhan, Eric Smith, Javier Rando, Yiming Zhang, Kate Plawiak, Zacharie Delpierre Coudert, Kartikeya Upasani, and Mahesh Pasupuleti. 2024. Llama guard 3 vision: Safeguarding human-ai image understanding conversations. <i>arXiv preprint arXiv:2411.10414</i> .	728
675		729
676		730
677		
678		
679		
680	Paul F Christiano, Jan Leike, Tom Brown, Miljan Martic, Shane Legg, and Dario Amodei. 2017. Deep reinforcement learning from human preferences. <i>Advances in neural information processing systems</i> , 30.	731
681		732
682		733
683		734
684	Karl Cobbe, Vineet Kosaraju, Mohammad Bavarian, Mark Chen, Heewoo Jun, Lukasz Kaiser, Matthias Plappert, Jerry Tworek, Jacob Hilton, Reiichiro Nakano, Christopher Hesse, and John Schulman. 2021. Training verifiers to solve math word problems. <i>arXiv preprint arXiv:2110.14168</i> .	735
685		736
686		737
687		
688		
689		
690	Corinna Cortes and Vladimir Vapnik. 1995. Support-vector networks. <i>Machine learning</i> , 20(3):273–297.	738
691		739
692		740
693		741
694		742
695	Justin Cui, Wei-Lin Chiang, Ion Stoica, and Chou-Jui Hsieh. 2025. Or-bench: An over-refusal benchmark for large language models. <i>Preprint</i> , arXiv:2405.20947.	743
696		744
697		745
698		
699		
700	William B Dolan and Chris Brockett. 2005. Automatically constructing a corpus of sentential paraphrases. In <i>Proceedings of the International Workshop on Paraphrasing</i> .	746
701		747
702		748
703		749
704		750
705	Nelson Elhage, Tristan Hume, Catherine Olsson, Nicholas Schiefer, Tom Henighan, Shauna Kravec, Zac Hatfield-Dodds, Robert Lasenby, Dawn Drain, Carol Chen, and 1 others. 2022. Toy models of superposition. <i>arXiv preprint arXiv:2209.10652</i> .	751
706		
707		
708		
709		
710	Clémentine Fourrier, Nathan Habib, Alina Lozovskaya, Konrad Szafer, and Thomas Wolf. 2024. Open Ilm leaderboard v2. <a href="https://huggingface.co/spaces/open-ilm-leaderboard/open_ilm_leaderboard">https://huggingface.co/spaces/open-ilm-leaderboard/open_ilm_leaderboard</a> .	752
711		753
712		754
713		755
714		756
715		757
716	Leo Gao, Jonathan Tow, Stella Biderman, Sid Black, Anthony DiPofi, Charles Foster, Laurence Golding, Jeffrey Hsu, Kyle McDonell, Niklas Muenninghoff, Jason Phang, Laria Reynolds, Eric Tang, Anish Thite, Ben Wang, Kevin Wang, and Andy Zou. 2021. A framework for few-shot language model evaluation.	758
717		759
718		760
719		
720		
721	Mor Geva, Roei Schuster, Jonathan Berant, and Omer Levy. 2021. Transformer feed-forward layers are key-value memories. In <i>Proceedings of the 2021 Conference on Empirical Methods in Natural Language Processing</i> , pages 5484–5495, Online and Punta Cana,	761
722		762
723		
724		
725		
726		
727		
728		
729		
730		
731	Dominican Republic. Association for Computational Linguistics.	731
732		732
733		733
734		734
735	Albert Q. Jiang, Alexandre Sablayrolles, Arthur Mensch, Chris Bamford, Devendra Singh Chaplot, Diego de las Casas, Florian Bressand, Gianna Lengyel, Guillaume Lample, Lucile Saulnier, Lélio Renard Lavaud, Marie-Anne Lachaux, Pierre Stock, Teven Le Scao, Thibaut Lavril, Thomas Wang, Timothée Lacroix, and William El Sayed. 2023. <i>Mistral 7b</i> . <i>Preprint</i> , arXiv:2310.06825.	735
736		736
737		737
738	Tom Kwiatkowski, Jennimaria Palomaki, Olivia Redfield, Michael Collins, Ankur Parikh, Chris Alberti, Danielle Epstein, Illia Polosukhin, Jacob Devlin, Kenton Lee, and 1 others. 2019. Natural questions: a benchmark for question answering research. <i>Transactions of the Association for Computational Linguistics</i> , 7:453–466.	738
739		739
740		740
741		741
742		742
743	Bruce W Lee, Inkit Padhi, Karthikeyan Natesan Ramamurthy, Erik Miehling, Pierre Dognin, Manish Nagireddy, and Amit Dhurandhar. 2024. Programming refusal with conditional activation steering. <i>arXiv preprint arXiv:2409.05907</i> .	743
744		744
745		745
746	Fan Liu, Zhao Xu, and Hao Liu. 2024a. Adversarial tuning: Defending against jailbreak attacks for llms. <i>arXiv preprint arXiv:2406.06622</i> .	746
747		747
748		748
749		749
750		750
751		751
752	Zihan Liu, Ruinan Zeng, Dongxia Wang, Gengyun Peng, Jingyi Wang, Qiang Liu, Peiyu Liu, and Wenhui Wang. 2024b. Agents4plc: Automating closed-loop plc code generation and verification in industrial control systems using llm-based agents. <i>arXiv preprint arXiv:2410.14209</i> .	752
753		753
754		754
755		755
756		756
757		757
758		758
759		759
760	Microsoft, :, Abdelrahman Abouelenin, Atabak Ashfaq, Adam Atkinson, Hany Awadalla, Nguyen Bach, Jianmin Bao, Alon Benhaim, Martin Cai, Vishrav Chaudhary, Congcong Chen, Dong Chen, Dongdong Chen, Junkun Chen, Weizhu Chen, Yen-Chun Chen, Yi ling Chen, Qi Dai, and 57 others. 2025. Phi-4-mini technical report: Compact yet powerful multimodal language models via mixture-of-loras. <i>Preprint</i> , arXiv:2503.01743.	760
761		761
762		762
763	OpenAI. 2024. Gpt-4 technical report. <i>Preprint</i> , arXiv:2303.08774.	763
764		764
765		765
766		766
767		767
768		768
769	Fabian Pedregosa, Gaël Varoquaux, Alexandre Gramfort, Vincent Michel, Bertrand Thirion, Olivier Grisel, Mathieu Blondel, Peter Prettenhofer, Ron Weiss, Vincent Dubourg, and 1 others. 2011. Scikit-learn: Machine learning in python. <i>the Journal of machine Learning research</i> , 12:2825–2830.	769
770		770
771		771
772	R. Penrose. 1955. A generalized inverse for matrices. <i>Mathematical Proceedings of the Cambridge Philosophical Society</i> , 51(3):406–413.	772
773		773
774	Ruchira Ray and Ruchi Bhalani. 2024. Mitigating exaggerated safety in large language models. <i>arXiv preprint arXiv:2405.05418</i> .	774

775	Paul Röttger, Hannah Rose Kirk, Bertie Vidgen, Giuseppe Attanasio, Federico Bianchi, and Dirk Hovy. 2024. <i>Xtest: A test suite for identifying exaggerated safety behaviours in large language models</i> . <i>Preprint</i> , arXiv:2308.01263.	829
776		830
777		831
778		832
779		
780	Leheng Sheng, Changshuo Shen, Weixiang Zhao, Jun-feng Fang, Xiaohao Liu, Zhenkai Liang, Xiang Wang, An Zhang, and Tat-Seng Chua. 2025. Alphasteer: Learning refusal steering with principled null-space constraint. <i>arXiv preprint arXiv:2506.07022</i> .	833
781		834
782		835
783		836
784		837
785	Richard Socher, Alex Perelygin, Jean Wu, Jason Chuang, Christopher D. Manning, Andrew Ng, and Christopher Potts. 2013. Recursive deep models for semantic compositionality over a sentiment treebank. In <i>Proceedings of the 2013 Conference on Empirical Methods in Natural Language Processing</i> , pages 1631–1642, Seattle, Washington, USA. Association for Computational Linguistics.	838
786		839
787		
788		
789		
790		
791		
792		
793	Nisan Stiennon, Long Ouyang, Jeffrey Wu, Daniel Ziegler, Ryan Lowe, Chelsea Voss, Alec Radford, Dario Amodei, and Paul F Christiano. 2020. Learning to summarize with human feedback. <i>Advances in neural information processing systems</i> , 33:3008–3021.	840
794		841
795		842
796		843
797		844
798		
799	Gemma Team. 2024a. <i>Gemma</i> .	845
800		846
801		847
802	Qwen Team. 2024b. <i>Qwen2.5: A party of foundation models</i> .	848
803		849
804	Qwen Team. 2025. <i>Qwen3 technical report</i> . <i>Preprint</i> , arXiv:2505.09388.	850
805		851
806	Alex Warstadt, Amanpreet Singh, and Samuel R. Bowman. 2018. Neural network acceptability judgments. <i>arXiv preprint 1805.12471</i> .	852
807		853
808		854
809		855
810		
811		
812		
813		
814	Adina Williams, Nikita Nangia, and Samuel Bowman. 2018. A broad-coverage challenge corpus for sentence understanding through inference. In <i>Proceedings of the 2018 conference of the North American chapter of the association for computational linguistics: human language technologies, volume 1 (long papers)</i> , pages 1112–1122.	856
815		857
816		858
817		859
818		860
819	Sophie Xhonneux, Alessandro Sordoni, Stephan Günemann, Gauthier Gidel, and Leo Schwinn. 2024. Efficient adversarial training in llms with continuous attacks. <i>Advances in Neural Information Processing Systems</i> , 37:1502–1530.	861
820		862
821		863
822		864
823		865
824		
825		
826	An Yang, Baosong Yang, Binyuan Hui, Bo Zheng, Bowen Yu, Chang Zhou, Chengpeng Li, Chengyuan Li, Dayiheng Liu, Fei Huang, Guanting Dong, Haoran Wei, Huan Lin, Jialong Tang, Jialin Wang, Jian Yang, Jianhong Tu, Jianwei Zhang, Jianxin Ma, and 40 others. 2024a. Qwen2 technical report. <i>arXiv preprint arXiv:2407.10671</i> .	866
827		867
828	Yifan Yang, Qiao Jin, Furong Huang, and Zhiyong Lu. 2024b. <i>Adversarial attacks on large language models in medicine</i> . <i>Preprint</i> , arXiv:2406.12259.	868

866           **A Angles between Answer Vectors and**  
867           **Benign Vectors**

868           As shown in Figure 9, the angles between the an-  
869           swer vectors and benign vectors of different LLMs  
870           are approximately  $90^\circ$ , indicating that they are  
871           nearly orthogonal.

872           **B Discussion on Layer Type Selection**

873           In Section 4.2, we mention that we treat both  
874           MLP and attention sublayers as “layers” for se-  
875           lection. This is because both types of sublayers  
876           contribute to the model’s internal representations  
877           and decision-making processes. Modifying either  
878           type can influence the model’s behavior regarding  
879           safety alignment. Besides, we conduct preliminary  
880           experiments to compare the combined score (Eq. 6)  
881           distributions of MLP and attention sublayers. The  
882           results are presented in Figure 10. The results show  
883           that both MLP and attention sublayers exhibit simi-  
884           lar contribution score distributions across different  
885           LLMs. Later layers tend to have higher contribu-  
886           tion scores, indicating their greater relevance to  
887           safety-related decisions. Therefore, we treat both  
888           MLP and attention sublayers equally in our layer  
889           selection process.

890           **C Additional Instructions on General**  
891           **Ability Datasets**

892           In this section, we provide detailed instructions on  
893           the general ability datasets used in our experiments.

- **Corpus of Linguistic Acceptability (COLA)** (Warstadt et al., 2018) is a dataset for evaluating the grammatical acceptability of sentences. Each sample consists of a sentence and a binary label indicating whether the sentence is grammatically acceptable or not.
- **Multi-Genre Natural Language Inference (MNLI)** (Williams et al., 2018) is a large-scale dataset for natural language inference. Each sample consists of a pair of sentences annotated with textual entailment labels.
- **Recognizing Textual Entailment (RTE)** (Bentivogli et al., 2009) is a dataset for evaluating the ability of models to recognize textual entailment. Each sample consists of a pair of sentences where one sentence is the premise and the other is the hypothesis.

- **Microsoft Research Paraphrase Corpus (MRPC)** (Dolan and Brockett, 2005) is a dataset for evaluating the ability of models to recognize paraphrases. Each sample consists of a pair of sentences extracted from online news sources, with human annotations indicating whether each pair is semantically equivalent or not.

- **Stanford Sentiment Treebank (SST)** (Socher et al., 2013) is a dataset for sentiment analysis. Each sample consists of a sentence and a binary label indicating whether the sentiment of the sentence is positive or negative.

- **GSM8K** (Cobbe et al., 2021) is a dataset for evaluating the mathematical reasoning ability of models. Each sample consists of a math word problem and its corresponding solution.

927           **D Details about Experimental Setup**

We implement LLM-VA with max iteration number  $T = 30$ . The final modified model is obtained by selecting the best model on the validation set during the iterations. The numbers of selected layers  $L_{select}$  of each model are shown in Table 3. For the SVM-based vector identification, we use the default regularization parameter  $C = 1.0$  from scikit-learn (Pedregosa et al., 2011). For baseline methods, we follow the original papers and use the default hyperparameters. If the original papers do not provide hyperparameter settings for certain models, we transfer the hyperparameters from similar models (e.g., models with the same architecture or in the same family). All experiments are conducted on  $2 \times 80$  GB A100 GPUs. We use the default generation configurations in Hugging Face Transformers<sup>9</sup> for base LLMs during inference. The temperature parameters of all models are set to 0.0 to ensure deterministic outputs. We use a fixed random seed of 42 for reproducibility across all experiments.

949           **E Details on Judge Model Selection**

As far as we know, Qwen3-Guard-Gen-8B (Zhao et al., 2025) is currently the only open-source LLM specifically designed to evaluate jailbreak and over-refusal behaviors. We also considered combining multiple judge models to realize the evaluation (e.g., LlamaGuard 3 (Chi et al., 2024) for jailbreak and OR-Judge (Zhang et al., 2025a) for over-

<sup>9</sup><https://huggingface.co/docs/transformers/index>

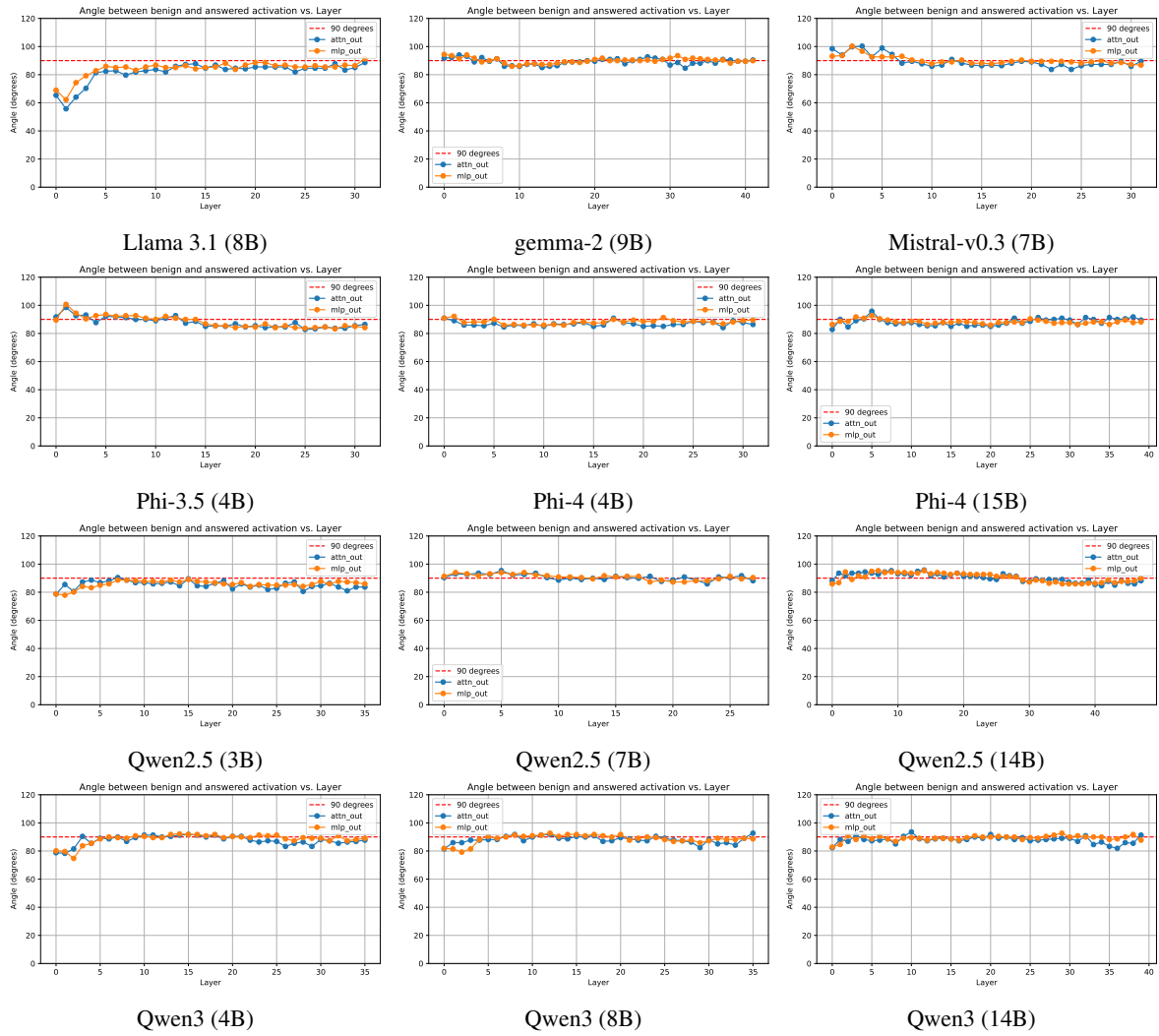


Figure 9: Angles between answer vectors and benign vectors of different LLMs.

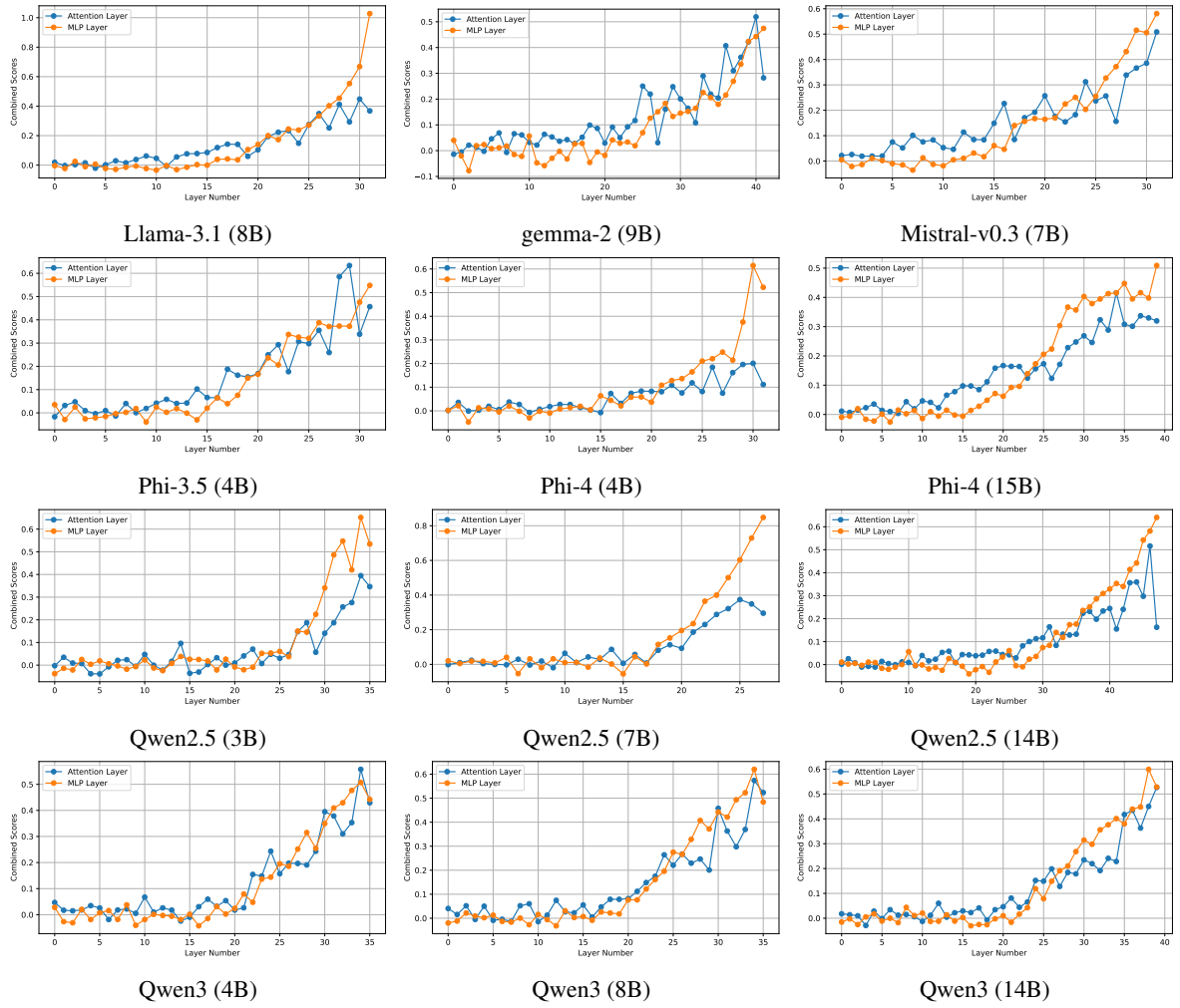


Figure 10: Comparison of combined scores between MLP and attention sublayers across different LLMs.

Table 3: Selected layer numbers of different models in LLM-VA.

Model	Llama-3.1	Gemma-2	Mistral-v0.3	Phi-3.5	Phi-4		Qwen2.5		Qwen3			
Size	8B	9B	7B	4B	4B	15B	3B	7B	14B	4B	8B	14B
# Selected Layers	42	60	42	30	48	54	60	36	54	48	60	48

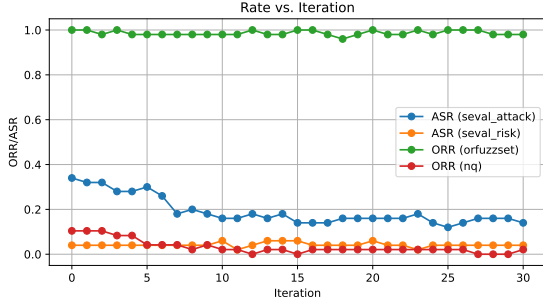


Figure 11: An example of evaluation results with combined judge models.

to improve the generalization of vector steering methods.

988  
989

refusal). However, due to their different judgement criteria, combining multiple judge models may lead to inconsistent evaluations. As a result, LLM-VA will find incorrect vectors to align, leading to suboptimal performance. Figure 11 shows an example of such inconsistent evaluations. The ORR evaluated by OR-Judge reaches 100% due to the inconsistency between the two judge models. Therefore, we choose Qwen3-Guard-Gen-8B as the sole judge model for a consistent evaluation of both jailbreak and over-refusal behaviors.

## F Detailed Results on Iteration Number

The detailed results on the impact of iteration number of each LLM are shown in Figure 12.

## G Transferability Experiments

To evaluate the transferability of LLM-VA, we assess how well the vector alignment learned on the training datasets generalizes to unseen datasets. We evaluate the modified models on three additional jailbreak datasets (XSTest-Toxic (Röttger et al., 2024), OR-Bench-Toxic (Cui et al., 2025), and AdvBench (Zou et al., 2023b)) and two over-refusal datasets (XSTest (Röttger et al., 2024) and OR-Bench (Cui et al., 2025)) that are not included in the training set. The results are shown in Table 4.

The results show that the performance of LLM-VA on unseen datasets varies across different models. While LLM-VA maintains reasonable safety alignment on most unseen datasets, the performance degradation compared to the training datasets indicates that further research is needed

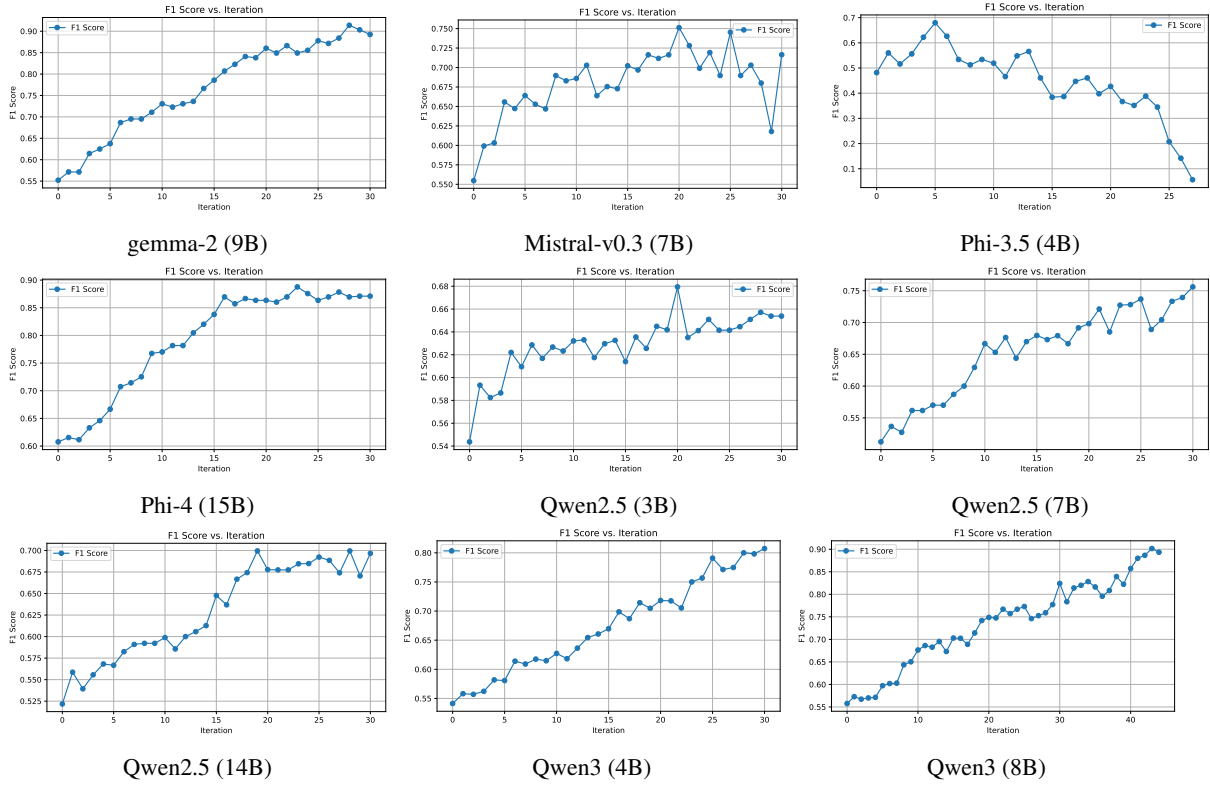


Figure 12: Detailed results on the impact of iteration number of each LLM.

Table 4: Transferability results on unseen datasets.

Model	Size	Method	AdvBench ASR↓	OR-Bench-Toxic ASR↓	XSTest-Toxic ASR↓	OR-Bench ORR↓	XSTest ORR↓	Final F1↑	Model	Size	Method	AdvBench ASR↓	OR-Bench-Toxic ASR↓	XSTest-Toxic ASR↓	OR-Bench ORR↓	XSTest ORR↓	Final F1↑
Llama-3.1	8B	Original	0.58%	3.05%	<b>0.00%</b>	48.22%	16.57%	0.7077	3B	3B	Original	0.19%	2.29%	0.57%	55.42%	19.34%	0.6522
		AlphaSteer+	0.58%	3.05%	<b>0.00%</b>	48.67%	17.13%	0.7038			AlphaSteer+	<b>0.00%</b>	2.44%	<b>0.00%</b>	53.53%	21.55%	0.6649
		AlphaSteer	0.19%	1.37%	<b>0.00%</b>	61.87%	27.07%	0.5921			AlphaSteer	0.19%	1.53%	<b>0.00%</b>	59.97%	21.55%	0.6144
		Steer	<b>0.00%</b>	<b>0.15%</b>	<b>0.00%</b>	85.60%	49.17%	0.3163			Steer	<b>0.00%</b>	<b>0.15%</b>	<b>0.00%</b>	85.97%	37.57%	0.3313
		SCANS	0.19%	1.37%	<b>0.00%</b>	72.48%	26.52%	0.4945			SCANS	6.35%	16.64%	1.15%	<b>40.11%</b>	<b>13.81%</b>	<b>0.7305</b>
		Modified	7.69%	5.80%	4.02%	<b>46.85%</b>	<b>6.63%</b>	<b>0.7088</b>			Modified	0.38%	4.12%	0.57%	54.21%	21.55%	0.6555
gemma-2	9B	Original	0.58%	1.98%	<b>0.00%</b>	80.52%	28.73%	0.4059	7B	7B	Original	<b>0.38%</b>	6.72%	<b>0.00%</b>	24.64%	8.84%	0.8569
		AlphaSteer+	0.77%	0.92%	0.57%	81.58%	<b>26.52%</b>	0.3985			AlphaSteer+	0.77%	6.11%	<b>0.00%</b>	24.87%	8.84%	0.8563
		AlphaSteer	<b>0.00%</b>	<b>0.46%</b>	<b>0.00%</b>	88.86%	28.73%	0.3103			AlphaSteer	3.08%	<b>3.66%</b>	<b>0.00%</b>	34.50%	9.39%	0.8006
		Steer	<b>0.00%</b>	<b>0.31%</b>	<b>0.00%</b>	94.16%	56.35%	0.1882			Steer	8.65%	5.50%	<b>0.00%</b>	61.03%	29.28%	0.5776
		SCANS	3.08%	5.50%	0.57%	<b>59.82%</b>	29.28%	<b>0.5952</b>			SCANS	1.54%	6.87%	1.72%	40.56%	11.60%	0.7552
		Modified	2.88%	1.68%	<b>0.00%</b>	82.41%	29.83%	0.3809			Modified	3.65%	9.92%	<b>0.00%</b>	<b>19.94%</b>	<b>7.73%</b>	<b>0.8714</b>
Mistral-v0.3	7B	Original	54.42%	48.70%	16.67%	<b>7.28%</b>	<b>3.87%</b>	0.7920	14B	14B	Original	<b>0.00%</b>	4.58%	<b>0.00%</b>	21.15%	8.29%	0.8816
		AlphaSteer+	52.12%	48.85%	16.67%	7.35%	4.42%	0.7937			AlphaSteer+	0.19%	5.34%	<b>0.00%</b>	20.77%	8.29%	0.8817
		AlphaSteer	45.38%	48.09%	14.37%	7.66%	4.97%	<b>0.8021</b>			AlphaSteer	0.00%	3.21%	<b>0.00%</b>	26.31%	9.39%	0.8551
		Steer	42.69%	40.92%	5.75%	11.75%	11.05%	0.7970			Steer	<b>0.00%</b>	<b>0.15%</b>	<b>0.00%</b>	57.01%	16.02%	0.6477
		SCANS	74.42%	41.98%	22.99%	18.57%	7.73%	0.7209			SCANS	7.88%	16.95%	2.30%	30.40%	19.34%	0.7824
		Modified	<b>27.31%</b>	<b>17.25%</b>	<b>2.87%</b>	37.30%	10.50%	0.7195			Modified	0.77%	5.04%	<b>0.00%</b>	<b>17.74%</b>	<b>6.08%</b>	<b>0.8990</b>
Phi-3.5	4B	Original	2.12%	4.89%	1.72%	45.49%	13.26%	0.7234	4B	4B	Original	0.96%	4.73%	0.57%	44.35%	6.63%	0.7402
		AlphaSteer+	<b>1.15%</b>	4.43%	1.15%	43.90%	13.81%	<b>0.7365</b>			AlphaSteer+	7.88%	24.58%	4.02%	<b>21.08%</b>	<b>4.42%</b>	<b>0.8307</b>
		AlphaSteer	<b>1.15%</b>	3.66%	1.15%	48.98%	13.81%	0.7022			AlphaSteer	33.85%	37.10%	8.62%	22.14%	7.73%	0.7634
		Steer	<b>1.15%</b>	3.51%	1.15%	56.41%	22.10%	0.6373			Steer	<b>0.77%</b>	<b>1.83%</b>	<b>0.00%</b>	66.49%	19.89%	0.5583
		SCANS	1.54%	<b>1.37%</b>	1.15%	79.83%	37.57%	0.3994			SCANS	3.65%	6.11%	0.57%	46.93%	11.60%	0.7107
		Modified	6.54%	6.41%	<b>0.00%</b>	<b>43.21%</b>	<b>12.71%</b>	0.7306			Modified	2.31%	4.27%	0.57%	36.69%	7.73%	0.7880
Phi-4	4B	Original	0.58%	2.14%	<b>0.00%</b>	58.83%	17.68%	0.6265	8B	8B	Original	0.96%	3.21%	1.15%	44.12%	9.39%	0.7419
		AlphaSteer+	<b>0.19%</b>	<b>1.53%</b>	<b>0.00%</b>	59.97%	18.23%	0.6182			AlphaSteer+	7.31%	14.20%	7.47%	62.70%	22.10%	0.5560
		AlphaSteer	<b>0.19%</b>	<b>1.53%</b>	<b>0.00%</b>	55.42%	18.23%	0.6551			AlphaSteer	<b>0.58%</b>	4.89%	1.15%	<b>34.65%</b>	<b>7.18%</b>	<b>0.8025</b>
		Steer	<b>0.19%</b>	2.60%	<b>0.00%</b>	46.70%	16.57%	0.7201			Steer	0.96%	4.12%	0.57%	40.03%	9.39%	0.7677
		SCANS	10.19%	12.98%	0.57%	36.01%	<b>8.84%</b>	0.7621			SCANS	<b>0.58%</b>	<b>2.29%</b>	<b>0.00%</b>	70.96%	20.99%	0.5147
		Modified	0.58%	7.63%	1.15%	<b>18.73%</b>	11.60%	<b>0.8841</b>			Modified	0.96%	3.82%	<b>0.00%</b>	40.71%	8.29%	0.7651
Phi-4	15B	Original	0.19%	3.97%	<b>0.00%</b>	72.71%	17.13%	0.5007	8B	8B	Original	0.19%	4.43%	0.57%	40.33%	7.18%	0.7683
		AlphaSteer+	<b>0.00%</b>	3.97%	<b>0.00%</b>	72.63%	15.47%	0.5039			AlphaSteer+	5.96%	22.44%	3.45%	<b>13.65%</b>	6.63%	<b>0.8743</b>
		AlphaSteer	<b>0.00%</b>	3.36%	<b>0.00%</b>	75.97%	16.57%	0.4704			AlphaSteer	0.77%	12.21%	0.57%	20.09%	<b>5.52%</b>	0.8719
		Steer	<b>0.00%</b>	<b>2.29%</b>	<b>0.00%</b>	84.23%	20.99%	0.3762			Steer	<b>0.00%</b>	<b>0.31%</b>	0.57%	72.33%	20.99%	0.5052
		SCANS	1.35%	5.95%	<b>0.00%</b>	67.78%	<b>11.60%</b>	0.5490			SCANS	29.04%	26.11%	9.20%	35.94%	25.41%	0.6955
		Modified	0.77%	3.82%	<b>0.00%</b>	<b>53.37%</b>	<b>11.60%</b>	<b>0.6727</b>			Modified	4.81%	3.05%	<b>0.00%</b>	51.86%	11.05%	0.6801